JOURNAL OF GUIDANCE, CONTROL, AND DYNAMICS
Vol. 19, No. 2, March–April 1996

Advanced Helicopter Flight Control Using Two-Degree-of-Freedom H^∞ Optimization

D. J. Walker and I. Postlethwaite
Leicester University, Leicester LE1 7RH, England, United Kingdom

We report on the design and ground-based piloted simulation testing of a high-performance helicopter flight control system. An observer-based multivariable controller was designed using a singular-value loop shaping method based on a two-degree-of-freedom H^∞ optimization, formulated to give robust model following and stability. The controller provided wide envelope stability and almost total decoupling, consistently allowing level-1 Cooper–Harper handling qualities ratings to be achieved for mission task elements performed on the large motion simulator at the Defence Research Agency, Bedford, England. Although designed for hover and low speed, it was successfully tested at speeds of up to 90 kn. In the words of one of the test pilots, the controller performed outstandingly.

Introduction

THE continuing drive to extend the operational capabilities of combat helicopters will require flight control systems with handling qualities tailored to the mission task. By removing the pilot from low-level stabilization and control loops, there will be considerable scope for improved mission effectiveness and survivability, particularly when required to operate in adverse conditions.

The vehicle of interest is the Westland Lynx multirole combat helicopter. This type of helicopter presents pilots with a high workload. It is open-loop unstable and exhibits high levels of cross coupling and variations in handling characteristics with flight condition. Use of automatic control for stabilization and reduction of cross coupling is standard in this type of aircraft, although the controllers tend to be low authority. That is, most of the available actuator authority—typically 80% or more—is directly in the hands of the pilot.

In 1988, as part of an earlier collaboration with the then Royal Aerospace Establishment (RAE), Yue and Postlethwaite[1] demonstrated the potential of H^∞ optimal control theory for the design of full authority helicopter flight control systems. They tested successfully using the ground-based facilities at RAE Bedford, now the Defence Research Agency (DRA), an 18-state control law designed for hover/low speed. This led to the first piloted simulation of a rotorcraft controller designed using H^∞ optimization. Other work based on the Lynx can be found in Refs. 2–4. In Ref. 2, the authors used a one-degree-of-freedom (1-DOF) H^∞ loop shaping procedure. In Ref. 4, the design and evaluation are described of a linear quadratic Gaussian/loop transfer recovery controller for a 30-kn trim condition. That work did not, however, make use of nonlinear models or piloted simulations for the evaluation. The aim of this paper is to describe how better performance was achieved over a wide range of simulated flight condition, using the most accurate nonlinear models available. Piloted simulation was a vital part of this work, as was determining compliance with the Military Rotorcraft Handling Qualities Specification.[5] The main contribution is the design of a novel multivariable controller giving high performance and robust stability. We demonstrate how specified quantitative handling qualities requirements can be incorporated into the design process. Results are presented from piloted simulations using one of the world's most advanced simulation facilities: the large motion simulator (LMS) at DRA Bedford.

Objectives

The basic aim of this research was to investigate ways of designing a high-bandwidth full-authority controller and to investigate

Daniel Walker received his B.A. degree in Engineering Science (Mechanical) from Oxford University in 1985 and a Ph.D. in Electrical Engineering (Control) from Imperial College in 1992. He was a visiting scholar at Moscow State University in 1987. From 1989 to 1992 he was a Research Associate at Leicester University Engineering Department working on Helicopter Flight Control. He is currently a Lecturer in Mechanisms and Control at Leicester. His research interests include Robust Control and its applications in Electrical and Mechanical Engineering.

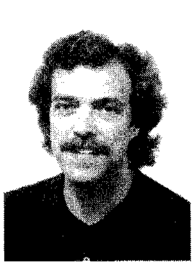

Ian Postlethwaite received his B.Sc. (Engineering) degree from Imperial College in 1975 and Ph.D. degree from Cambridge University in 1978. After a Research Fellowship at Cambridge University and a Lectureship at Oxford University in 1988 he was appointed to a Chair of Engineering at Leicester University. His current research interests include robust control, optimal control and the application of advanced control system design to real engineering systems. He is a Fellow of the Institution of Electrical Engineers and a Senior Member of the Institute of Electrical and Electronics Engineers.

Received Feb. 23, 1995; revision received Aug. 11, 1995; accepted for publication Sept. 11, 1995. Copyright © 1995 by D. J. Walker and I. Postlethwaite. Published by the American Institute of Aeronautics and Astronautics, Inc., with permission.

the interactions between the controller and the aircraft's dynamics within the constraints of the available model. Of interest were 2-DOF controllers. The controller was to provide robust stability and a suitable response type, enabling the aircraft to be flown with a low workload. An attitude-command, attitude-hold (ACAH) response type was specified whereby the pilot would demand pitch attitude (θ), roll attitude (ϕ), heading rate ($d\psi/dt$), and heave velocity (dh/dt), all measured with respect to an Earth-based frame of reference. These measurements, together with the body-axis pitch and roll rates (q and p, respectively), were assumed to be available to the controller.

ADS-33C Handling Qualities Requirements

ADS-33C (Ref. 5) represents the latest specification for combat helicopters and is intended to ensure that mission effectiveness is not compromised by deficient handling qualities. The specification states that "compliance with the requirements will be demonstrated using analysis, simulation and flight-test at appropriate milestones during the rotorcraft design and development." The requirements are stated in terms of three limiting levels of acceptability of one or more given parameters. The levels indicate performance attributes that equate to pilot ratings on the Cooper–Harper scale. Qualitative descriptions of the three levels can be summarized as level 1, satisfactory without improvement; level 2, adequate performance attainable with tolerable workload, deficiencies warrant improvement; and level 3, adequate performance is unattainable with tolerable workload, deficiencies require improvement. To assess the designs prior to piloted testing in the simulator, compliance with a subset of the quantitative requirements in ADS-33C specification was determined. A Handling Qualities Toolbox[6] was used to help integrate handling qualities assessment into the complete design and analysis cycle. Piloted simulation was later used that allowed test pilots to rate the control law on the basis of its performance during a number of simulated ADS-33C-style mission task elements.

H^∞ Optimal Control Theory

H^∞ optimization provided the basic design methodology. An introduction to the theory is given by Francis.[7] Figure 1 depicts the standard problem in H^∞ control, in which w, u, z, and y are vector-valued signals: w is the exogenous input, consisting of commands, disturbances, sensor noise, and the like; u the control input; z the controlled output consisting of errors, actuator signals, or, as depicted, inputs to perturbation models; and y the measurement. $P(s)$ is partitioned conformably with its two inputs (w and u) and its two outputs (z and y). $K(s)$ is a linear time-invariant controller. Δ represents model uncertainty. Thus, Fig. 1 stands for the equations

$$\begin{bmatrix} z \\ y \end{bmatrix} = \begin{bmatrix} P_{11} & P_{12} \\ P_{21} & P_{22} \end{bmatrix} \begin{bmatrix} w \\ u \end{bmatrix} \tag{1}$$

$$u = Ky \tag{2}$$

Eliminating u and y, one finds (for $\Delta = 0$) that the closed-loop transfer function from w to z, denoted T_{zw}, is given by

$$T_{zw} = P_{11} + P_{12}K(I - P_{22}K)^{-1}P_{21} \tag{3}$$

The H^∞ norm of the stable transfer function matrix $F(s)$, denoted $\|F\|_\infty$, is defined as

$$\|F\|_\infty := \sup\{\sigma_{\max}[F(j\omega)]: 0 \le \omega \le \infty\} \tag{4}$$

where $\sigma_{\max}$ denotes the maximum singular value. The standard problem in H^∞ control is to synthesize a stabilizing $K(s)$ that minimizes the H^∞ norm of the closed-loop transfer function from disturbance input w to the output z; that is, that minimizes $\|T_{zw}\|_\infty$ over all stabilizing $K(s)$. The L_2 norm of the signal $w(t)$ is defined as

$$\|w(t)\|_2 := \sqrt{\left(\int_0^\infty w'(t)w(t)\,dt\right)} \tag{5}$$

when the integral exists (w' denotes the transpose of w). The square of the L_2 norm of $w(t)$ is sometimes referred to as the energy in

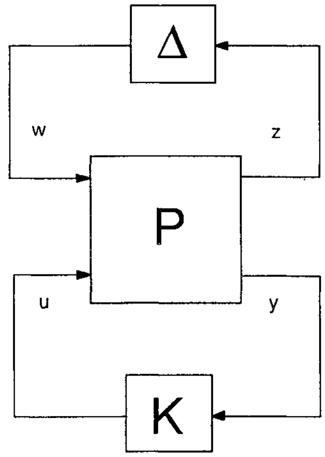

Fig. 1 H_∞ regulator with perturbation.

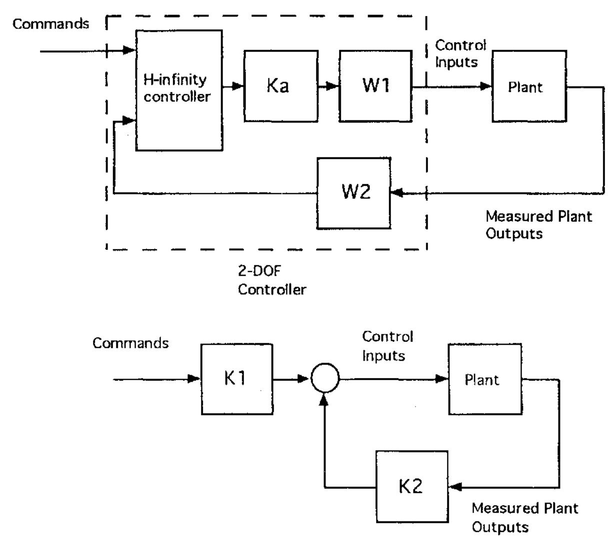

Fig. 2 Two-DOF control.

$w(t)$. A controller that minimizes the H^∞ norm of the closed-loop transfer function T_{zw} minimizes the worst-case L_2 norm of $z(t)$ over all $w(t)$ of given L_2 norm: that is, it minimizes the energy gain from w to z.

Suppose $K(s)$ internally stabilizes the nominal ($\Delta = 0$) system $P(s)$ in Fig. 1: i.e., T_{zw} is internally stable. The small gain theorem states that the perturbed system will remain stable in the face of any stable perturbation $\{\Delta: \|\Delta\|_\infty \le 1\}$ if and only if $\|T_{zw}\|_\infty < 1$. Thus, given nominal stability, the condition $\|T_{zw}\|_\infty < 1$ is equivalent to robust stability in the presence of any Δ in the class defined (in practice, not all of these perturbations will be physically meaningful; hence, the inherent conservatism in singular valued based robustness tests).

2-DOF Control

Control problems often possess 2-DOF, associated with availability of feedback signals, on the one hand, and of set points or references on the other: in this context, demands in θ, ϕ, $d\psi/dt$, and dh/dt from the pilot. A generic 2-DOF feedback control loop is depicted in Fig. 2. References and feedback signals all enter the controller separately where they are used to generate control signals. The 2-DOF controller is equivalent to a command path filter K_1 and a feedback compensator K_2 (see Fig. 2). Within a 2-DOF framework, robustness and other properties of the feedback loop can be decoupled from closed-loop command-following properties.[8] In the design presented here, a simple idealized step response model (SRM) that encapsulated basic handling requirements was employed. H^∞ optimization was then used to synthesize a controller that forced the closed loop to approximate the SRM accurately by reducing the H^∞ norm of the error between the two.

Table 1 Rotor parameters

Regressing flap mode	$\zeta = 0.5987$, $\omega_0 = 13.4720$ rad/s
Advancing flap mode	$\zeta = 0.2154$, $\omega_0 = 68.7376$ rad/s
Coning mode	$\zeta = 0.4032$, $\omega_0 = 37.6518$ rad/s

Aircraft Simulation Model

The basis for the design was the DRA rationalized helicopter model[9] (RHM). This is a nonlinear model configured to represent the Lynx. It comprises various interacting modules simulating rigid body, actuator, engine, and rotor dynamics. Sensor dynamics, although available, were not used in this work. Separate aerodynamic force and moment contributions of the main rotor, tail rotor, fuselage, fin, and horizontal stabilizer were modeled, with the main rotor model consisting of rigid constant chord blades hinged with stiffness in flap at the center of rotation. The model includes nonuniform induced flow, but a constant lift slope is assumed and unsteady aerodynamic effects are ignored. A third-order engine model provided torque and rotor speed characteristics. The four main actuators were modeled using first order lags with position and rate limits. The time constants were of the order of 0.1 s and rate limits were between 20 and 80 deg/s. The RHM reproduces most of the characteristics of the Lynx. Correlation with flight data is good, and qualitative pilot comment favorable.[10] It was used for both off-line analysis and piloted simulation, as well as providing the linearization for controller synthesis. The design was based on a linearization taken at hover and containing eight rigid-body states and four actuator states, partly to test the hypothesis that a low-order model would be adequate for design purposes, provided due attention was paid to robustness.

Model Uncertainty and Rotor Modes

Various methods exist for expressing model error bounds. Gain and phase margins are widely used as measures of the additional amount of pure gain and pure phase that can be tolerated in a single-input single-output (SISO) feedback loop without loss of stability. These margins can easily lead to erroneous conclusions, especially when applied to multivariable systems, as indeed they commonly are. Singular value Bode plots provide the means of determining robustness to unstructured plant perturbation in multivariable feedback loops, although the tests may be highly conservative. In this design example, the absence of hard information regarding the structure and distribution of model error made the use of singular value techniques natural. The main rotor exhibits oscillatory flapping, coning, and lead-lag modes. The RHM included a fully coupled sixth-order model of coning and flapping, but the lag mode was not modeled at that time. Flapping and coning modes were characterized in the design linearization by complex poles with the damping factors and natural frequencies given in Table 1.

The lag mode is likely to be more lightly damped and of lower natural frequency than the modes in Table 1. With real-time simulation facilities at DRA Bedford then operating at a 20-ms frame time, it was impossible to simulate coning and flapping in real time. A quasisteady rotor model was therefore used in piloted tests. This, together with the absence of sensor dynamics, means that significant model uncertainty exists at frequencies above 9 or 10 rad/s. The model with sixth-order flapping and coning was used in all off-line simulations and for assessing quantitative compliance with ADS-33C criteria. Robustness to both modeled and unmodeled rotor dynamics was aimed for by guaranteeing adequate attenuation in the loop gain at mid to high frequencies, where rotor effects become pronounced.

Controller Design

The method adopted for the design of the controller was proposed in Ref. 11. It is essentially an extension of the multivariable loop shaping design procedure of McFarlane and Glover,[12] the main difference being that the additional DOF is used to force the behavior of the closed loop system to approximate closely that of a specified SRM. The design process consists of first augmenting the open-loop plant, and then performing a multiobjective H^∞ optimization. The design method uses a normalized coprime factor description of the augmented plant. $[N\ M]$ denotes a left coprime factorization of the nominal augmented plant transfer function matrix $G(s)$ (assumed given). This means that $G = M^{-1}N$, in which N and M are stable, and there is no cancellation of any unstable dynamics between M^{-1} and N. The factorization is said to be normalized if, in addition, $[N\ M]$ is all-pass.

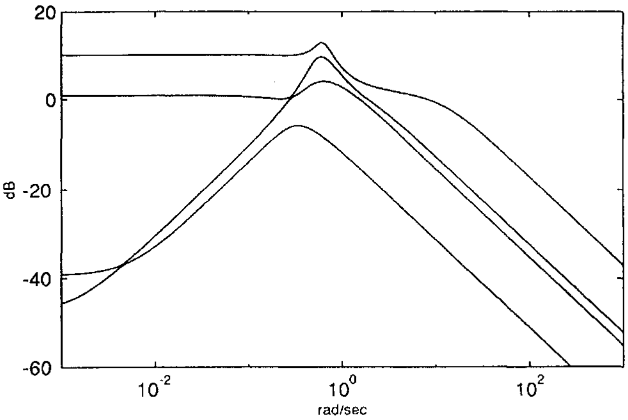

Fig. 3 Singular values of the unaugmented model at hover.

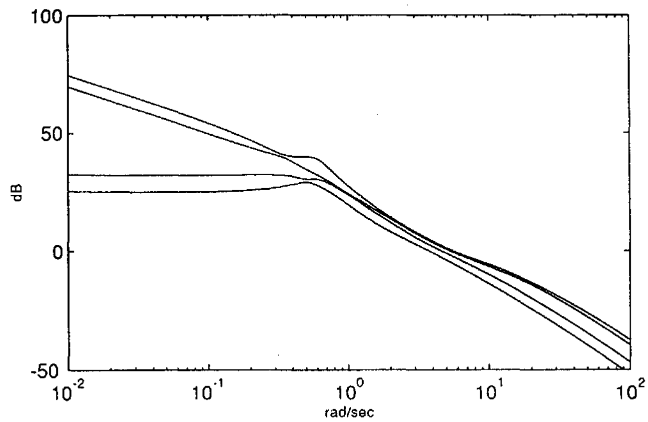

Fig. 4 Singular values of the augmented model at hover.

Weighting Function Selection

Before shaping, plant outputs were normalized as described in Ref. 1. Shaping was then carried out, using a frequency-dependent weight on the input and a constant weight on the output. The philosophy behind the shaping process is described in Ref. 12. Six variables were fed back to the controller via the constant weight $W_2(s)$ (see Fig. 2): heave velocity, pitch and roll attitudes, and heading rate, together with body-axis pitch and roll rates

Inspection of the singular values of the unaugmented model (Fig. 3) reveals low dc gain in two channels and a poor condition number. The following prefilter $W_1(s)K_a$ and postfilter $W_2(s)$ were cascaded with the plant:

$$W_1(s) = \mathrm{diag}\begin{bmatrix} \frac{s+5}{s} & \frac{s+5}{s} & \frac{s+5}{s} & \frac{s+5}{s} \end{bmatrix} \tag{6}$$

$$W_2(s) = \mathrm{diag}(1.0 \quad 1.0 \quad 1.0 \quad 1.0 \quad 0.5 \quad 0.5) \tag{7}$$

$$K_a = \mathrm{align}[W_2 G(j5.0) W_1(j5.0)] \tag{8}$$

These filters are all shown in Fig. 2. W_1 is essentially a proportional-plus-integral filter, used to boost the low-frequency gain in all channels; the zero was used in each channel to reduce the rolloff close to gain crossover that is set to around 5 rad/s using an alignment gain K_a obtained at this frequency. The alignment algorithm[13] calculates an approximate plant inverse at the desired frequency and can be used to set the 0-dB crossover. Note that the plant is considerably better conditioned at 5 rad/s than it is at dc. The output weight W_2 feeds back in equal proportion each of the four controlled outputs. The

Table 2 Relationship between γ_{opt} and ρ

ρ	0	0.1	0.2	0.4	0.75	1.0	1.5	2.0	3.0
γ_{opt}	2.89	2.90	2.92	2.99	3.23	3.46	3.98	4.59	6.35

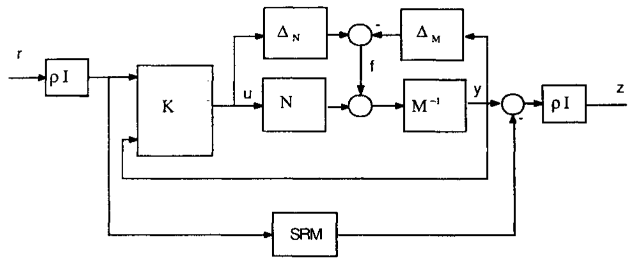

Fig. 5 Optimization structure.

relative weighting of 50% on the body-axis rates p and q is designed to desensitize the error signal with respect to these signals, although still making them available for stabilization purposes. The singular values of the shaped plant are shown in Fig. 4. Note the attenuation in the specified loop gain at frequencies beyond about 7 rad/s, where unmodeled rotor dynamics are liable to become significant.

H^∞ optimization was then applied to the shaped plant. Figure 5 shows the configuration used in the optimization. The SRM is selected so as to embody desired handling qualities.

Plant uncertainty is represented by Δ_N and Δ_M. The perturbed (shaped) plant transfer function is $(M + \Delta_M)^{-1}(N + \Delta_N)$. A controller is sought that robustly stabilizes $G(s)$ in the presence of perturbations Δ_N and Δ_M and simultaneously forces the worst-case L_2 norm of the weighted error (z) between the outputs of the plant and the SRM to be small. This forces the closed-loop system to resemble the SRM. H^∞ optimization was used to synthesize a stabilizing controller that reduced the H^∞ norm of the closed-loop transference from (r, f) to (u, y, z) close to the minimum theoretically achievable: the H^∞ optimal cost γ_{opt}. The vector-valued signals r, f, u, and y are the reference, the disturbance, the control, and the (shaped) plant output, respectively. The scalar ρ weights model following in the optimization. For instance, $\rho = 0$ places zero weighting on model following, and results simply in robust stability. Better model following tends to be at the expense of robustness, as seen by the increased H^∞ optimal cost γ_{opt} shown in Table 2. A value for $\rho = 1.5$ was chosen to give satisfactory model following, and a 27-state controller was obtained. This guarantees a 25% margin for error on the nominal shaped plant coprime factorization.

Analysis in Ref. 14 has shown that an admissible controller can be realized by a system combining an observer, the dynamics of the SRM, and a state (estimate) feedback law. This well-defined controller structure was exploited to design a scheduled control law that was also tested and that will be reported on separately.

Selection of SRM

The SRM defined the desired responses in heave, pitch, roll, and heading axes. In practice, any system with inertia will exhibit at least second-order response, with continuous angular and translational rates following a step demand. A second-order transfer function of the form

$$T(s) = \frac{\omega_n^2}{s^2 + 2\zeta\omega_n s + \omega_n^2} \tag{9}$$

was therefore used to define the desired response in each axis. A damping factor ζ of 0.9 was used in each axis. This meets level-1 damping requirements given in Sec. 3.3 of ADS-33C for midterm response in pitch and roll. The natural frequency ω_n was chosen to provide an adequate speed of responses in each axis. The parameters ζ and ω_n can be related to the moderate amplitude criteria of ADS-33C Sec. 3.3 that define agility. For instance, ADS-33C defines lower limits on the peak angular rate required to accomplish a given pitch or roll attitude change. The agility, defined as the ratio of peak angular rate to peak attitude response following a step input, is given by

$$\frac{\omega_n \exp(-\zeta/\sqrt{1-\zeta^2}) \arcsin\sqrt{1-\zeta^2}]}{1 + \exp(-\pi\zeta/\sqrt{1-\zeta^2})} \tag{10}$$

The SRM natural frequencies are summarized in Table 3. The rise time t_r is defined as the time to reach the first peak following a step input and is given by

$$t_r = \frac{\pi}{\omega_n\sqrt{1-\zeta^2}} \tag{11}$$

This leads to agilities of 1.42 and 2.85 Hz for pitch and roll axes and meets ADS-33C level-1 requirements over most of the attitude range. Results later obtained from nonlinear simulations verified this.

ADS-33C also defines bandwidth and phase-delay parameters (ω_{BW} and τ_P, respectively) relating to the small-amplitude short-term frequency responses. For an ACAH response type, these are defined in terms of the phase response alone. In terms of ζ and ω_n, ω_{BW} is given by

$$\omega_{BW} = \omega_n(\zeta + \sqrt{1+\zeta^2}) \tag{12}$$

Since the phase of the SRM is asymptotic to -180 deg, τ_P is undefined. Table 3 suggests that ω_{BW} in pitch and roll will be well inside the level-1 bounds; the fact that ω_{BW} is entirely dependent on phase meant that, in practice, the actual handling quality bandwidths, though still level 1, were somewhat lower.

Desirable heave response characteristics are defined in Sec. 3.3 of ADS-33C in terms of an equivalent first-order system with time constant T, cascaded with a pure delay Δ. The equivalent values for the SRM used, calculated in the manner prescribed in ADS-33C, were $T = 0.8225$ s and $\Delta = 0.162$ s. This satisfies level-1 criteria.

Time-Domain Analysis

The closed-loop step responses are shown in Figs. 6 and 7 for heave and pitch axes. These were obtained using the full nonlinear model, trimmed at the design operating point, with coning and flapping modes, rate-limited actuators, and engine dynamics. The tail rotor actuator rate limit was briefly reached during certain phases of some simulated maneuvers.

Table 3 SRM natural frequencies

Axis	Natural frequency ω_n, rad s^{-1}	Rise time t_r, s
Heave	2.059	3.5
Pitch	3.604	2.0
Roll	7.207	1.0
Heading	14.415	0.5

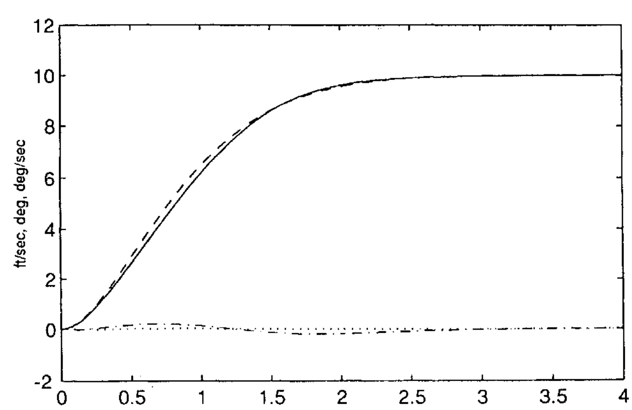

Fig. 6 Heave axis response (hover): ——, heave velocity; - - -, SRM for heave velocity; —·—, yaw rate; and ·····, pitch and roll attitude.

Table 4 Singular value robustness measures

Margins at		Guaranteed GM	Guaranteed PM, deg
Output	$\|(I - GK_2)^{-1}\|_\infty = 2.1088(6.48\,\text{dB})$	0.68–1.90	±27.4
Output	$\|GK_2(I - GK_2)^{-1}\|_\infty = 2.1719(6.74\,\text{dB})$	0.54–1.46	±26.6
Input	$\|(I - K_2G)^{-1}\|_\infty = 1.7993(5.1\,\text{dB})$	0.64–2.25	±32.3
Input	$\|K_2G(I - K_2G)^{-1}\|_\infty = 1.7411(4.82\,\text{dB})$	0.43–1.58	±33.4

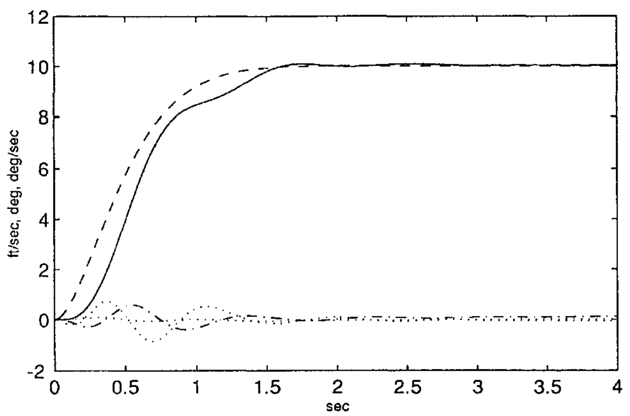

Fig. 7 Pitch axis response (hover): ——, pitch attitude; – – –, SRM for pitch attitude; —·—·, roll attitude; and ·····, heave and yaw rates.

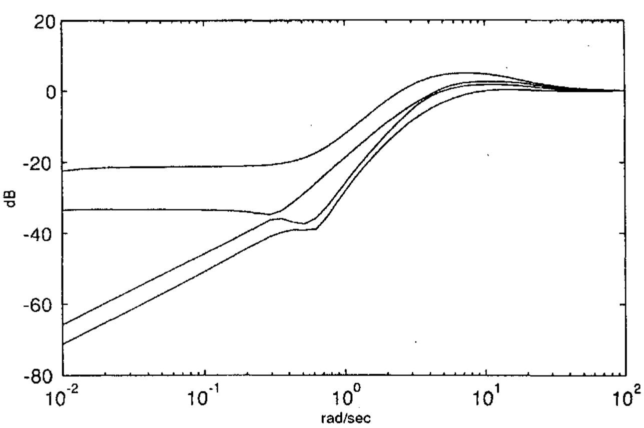

Fig. 8 Singular values of the input sensitivity, $S = (I - K_2G)^{-1}$.

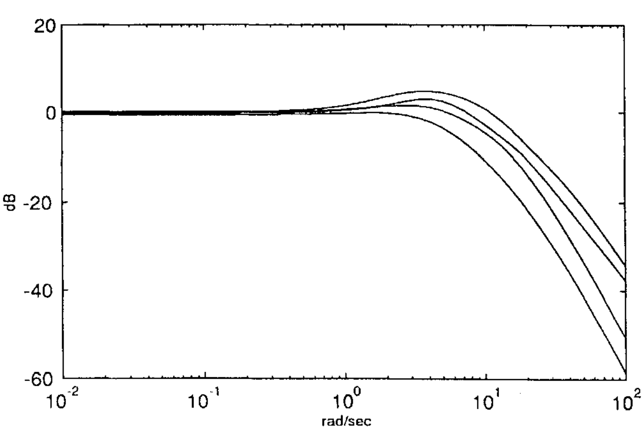

Fig. 9 Singular values of the input complementary sensitivity, $T = K_2G(I - K_2G)^{-1}$.

Frequency-Domain Analysis

The stability properties of the closed-loop system in the presence of unstructured stable additive and multiplicative perturbations Δ can be assessed in the frequency domain by considering appropriate closed-loop transfer functions. Figures 8 and 9 show singular value Bode plots of the input sensitivity and input complementary sensitivity functions. Output sensitivity and complementary sensitivity (not shown) are defined as $(I - GK_2)^{-1}$ and $GK_2(I - GK_2)^{-1}$, respectively. Guaranteed stability [gain margins (GM) and phase margin (PM)] at plant input (output) can be computed using the formulas[15]

$$1 - 1/\|T\|_\infty \le \text{guaranteed GM} \le 1 + 1/\|T\|_\infty \tag{13}$$

$$\text{guaranteed PM} = \pm 2\sin^{-1}(1/2\|T\|_\infty) \tag{14}$$

$$1/(1 + 1/\|S\|_\infty) \le \text{guaranteed GM} \le 1/(1 - 1/\|S\|_\infty) \tag{15}$$

$$\text{guaranteed PM} = \pm 2\sin^{-1}(1/2\|S\|_\infty) \tag{16}$$

where S and T are the sensitivity and complementary sensitivity at plant input (output). Table 4 gives these margins.

The figures in Table 4 are conservative. They represent the ranges of pure gain or phase that are allowed in each channel before a guarantee of stability is lost. Note that as with SISO margins, computed GM assume no phase change, and vice versa.

Handling Qualities Evaluation

The following analysis was made by applying criteria from ADS-33C to responses generated from the off-line model with full rotor and engine DOF. Results are presented for the hover flight condition.

Short-Term Frequency Responses

The ADS-33C bandwidth and phase-delay parameters Ω_{BW} and τ_P were computed via spectral analysis of the responses from the full nonlinear model to suitable test signals. The results are given in Table 5. All three axes meet level-1 criteria.

Midterm Response

To satisfy level-1 handling qualities criteria, a damping factor of at least 0.35 is required in pitch and roll axes. A damping of 0.9 was specified in the SRM. The values in Table 6 were calculated by analyzing the transient responses to pulse attitude demands in pitch and roll axes using the full nonlinear model trimmed at hover.

Table 5 Bandwidth and phase delay parameters

	Hover		50 kn	
Axis	ω_{BW}, rad/s	τ_P, s	ω_{BW}, rad/s	τ_P, s
Pitch	4.666	0.1281	5.083	0.1356
Roll	6.662	0.1333	7.412	0.1543
Yaw	4.536	0.0521	4.089	0.0122

Table 6 Damping factor of dominant poles at design operating point

Axis	Damping factor ζ
Pitch	0.82
Roll	0.96

Table 7 Pitch to roll coupling

Hover			50 kn		
θ_{max}, deg	ϕ_{max}, deg	ϕ_{max}/θ_{max}, %	θ_{max}, deg	ϕ_{max}, deg	ϕ_{max}/θ_{max}, %
5	0.29	5.7	5.1	0.44	8.6
15	0.87	5.8	15.5	1.36	8.8
25	1.5	5.7	26.0	2.31	8.9

Table 8 Roll to pitch coupling

Hover			50 kn		
ϕ_{max}, deg	θ_{max}, deg	θ_{max}/ϕ_{max}, %	ϕ_{max}, deg	θ_{max}, deg	θ_{max}/ϕ_{max}, %
10	0.13	1.38	10.2	0.07	0.7
30	0.56	1.84	30.1	0.39	1.3
40	1.04	2.57	39.9	0.90	2.3

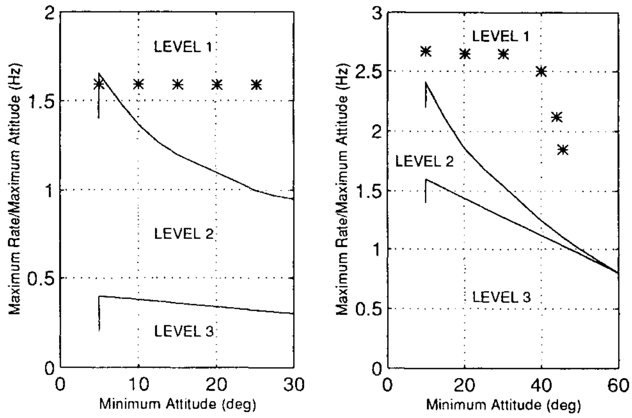

Fig. 10 Agility in pitch and roll (hover): pitch—combat/target track and roll—combat/target track

Moderate Amplitude Response

Compliance with the moderate amplitude criteria was assessed on pitch and roll axes using step inputs. The agility parameters as defined in ADS-33C for pitch and roll attitude changes are plotted in Fig. 10.

Interaxis Coupling

The ADS-33C level-1 requirement is that pitch-to-roll and roll-to-pitch coupling be less than 25%. The interaction levels are shown in Tables 7 and 8.

Piloted Trials

During 1992, two comprehensive piloted assessments were made at DRA Bedford. A crossfeed was implemented in the command path between the roll and yaw axes to give turn coordination above a preset forward velocity. The pilot could vary the amount of sideslip via his command inceptor. A Lynx-like single seat cockpit was used. This was mounted on the LMS. The motion system provides ±30 deg of pitch, roll, and yaw; ±4 m of sway; and ±5 m of heave motion. In piloted flight simulations, acceleration provides an important cue; the LMS can provide up to 10 m/s^2 in heave and up to 5 m/s^2 in sway or surge. Maximum angular accelerations about the pitch, roll, and yaw axes are 2, 3, and 1.5 rad/s^2, respectively. The pilot's seat was dynamically driven to give vibration and sustained normal acceleration cues. A three-axes side stick was used to control pitch, roll, and yaw, together with a conventional collective for heave. The visual display was generated by a Link–Miles IMAGE IV CGI system and gave approximately 48-deg field of view in pitch and 120 deg in azimuth, with full daylight texturing. Despite the obvious restrictions imposed by the limited depth of field and so forth, the visual database is enhanced with objects and texturing to such a degree that the usable cues available to the pilot are generally extremely good. A more detailed discussion of this, together with a full description of the LMS, can be found in Ref. 16.

Task Descriptions

Handling qualities were assessed for three hover/low-speed mission task elements (MTEs) (side step, quick hop, bob up) and three moderate/high-speed tasks (lateral jinking, hurdles, yaw pointing). These MTEs were considered appropriate to battlefield roles and adhere closely to the spirit of ADS-33C Sec. 4. The pitch and roll tasks were originally developed in flight trials and to maintain correspondingly representative control strategy, task aggression, and task performance, the simulation visual databases are enhanced with additional artificial cues. Both participating pilots had considerable experience of both the Lynx and the flight simulator. The criteria for adequate and desired performance, which were rigorously applied during the trials, were those used by the DRA. A detailed description of the manner in which piloted rotorcraft trials are conducted at DRA Bedford, including task performance requirements, is given by Padfield et al.[16] For most tasks, desired performance constituted heading control to within ±5 deg and position control to within ±2.5 m.

Task 1: Side Step

The objective was to translate sideways through 46 m from a hover at a height of 9 m above ground level in front of one diamond and square sighting arrangement and to acquire and maintain a stable hover in front of the next sighting system. Maintaining any two of the diamond points within the square satisfied the desired ±2.5-m lateral position and height tolerances. Task aggression was determined via initial bank angle, with 10, 20, and 30 deg, corresponding to low, moderate, and high levels of aggression.

Task 2: Quick Hop

The quick-hop task is the corresponding longitudinal task to the side step, requiring a reposition from hover over a distance of 150 m. Again, similar levels of initial pitch attitude were used to determine the task aggression. The task was flown down a walled alley to give suitable height and lateral position cues, and the terminal position tolerance was increased to ±9 m to allow for the reduced field of view over the nose.

Task 3: Lateral Jinking

The lateral jinking task concerned a series of S turns through slalom gates followed by a corresponding line tracking phase. The task had to be flown while maintaining a speed of 60 kn and a height of 8 m above ground level. Once more, bank angle was used to determine task aggression, with 15, 30, and 45 deg denoting low, moderate, and high levels of aggression. The width of the gates was determined by the adequate margin of performance for the tracking task (±6 m), with desired level being half of that.

Task 4: Hurdles

The hurdles task was flown as a collective-only flight-path repositioning task with a tracking phase. It was performed using several V-notch hurdles and flown at 60, 75, and 90 kn to represent increasing task aggression. From an initial height aligned with the bottom of the V notch, the pilot had to pass through each hurdle at the height denoted by black tips on the hurdle and then regain the original speed and height as quickly as possible. Although not a conventional flying strategy, both pilots adapted quickly. The desired performance was height of ±1.5 m during tracking, ±3 m during hurdle hop, and track ±6 m.

Task 5: Bob Up

Using the same V-notch hurdles as for task 4, from a hover aligned with the bottom of a V notch, the pilot had to acquire and maintain a new height denoted by the black tips. Task aggression was determined subjectively by the pilot based on magnitude of collective displacement. This gave a direct correlation with peak normal acceleration. The collective had been scaled so that maximum collective corresponded to the maximum allowable rate of climb.

Task 6: Yaw Pointing

While translating down the runway centerline at 60 kn, the pilot was required to yaw to acquire and track one of a number of offset posts in a sight. Task aggression was determined by the magnitude of the initial offset of the target. A heading control accuracy of approximately ±2 deg constituted desired performance. During this task, which is proposed in Ref. 17 as a severe robustness test for linear control laws, large lateral velocities and sideslips of 180 deg occurred.

For each task in turn, the pilot performed two or three familiarization runs before performing a definitive evaluation run, at the

Table 9

Task	Level of aggression	Pilot comment	HQR	Level
Quick hop	Low	Single-axis task. Task workload minimal. Desired performance achieved easily. Task cues artificial and specific, but good.	2	1
	High	Single-axis task. Slight coupling because of poor inceptor. Some deviation in lateral control because of limited lateral cues. Task workload between minimal and moderate. Desired performance achieved satisfactorily.	2	1
Side step	Low	Single-axis task, where this control law is absolutely outstanding. Task cues good. Desired performance easily achieved. Hands off the controls at hover. No tendency towards pilot-induced oscillations around hover. Responses very light and agile.	2	1
	High	Single-axis task. Using about 80% of helicopter's available performance. Desired performance easily achieved. Knowing when to put opposite input was only control problem. Very low workload for an aggressive task. Absolutely no problem to get desired tolerances.	2	1
Hurdles	Low	Task cues and field of view good. Good precision. Desired performance achieved satisfactorily. Some activity in all axes, but inputs very small. Task workload minimal.	2	1
Bob up	Moderate	Task cues good. Some yaw coupling, but within acceptable tolerance. Desired performance achieved satisfactorily. Task workload minimal. Peak torque 120% of rated.	2	1
	Moderate	(Pilot limiting torque to 100% rated. Torque displayed on head-up display.) All workload driven by monitoring torque. Desired performance achieved with some difficulty. Task workload: moderate to considerable.	4	2
Yaw pointing	Low	Precision good, no problem at all. Minimal control and workload. Desired performance achieved easily. Task cues good, scene content good, field of view adequate.	2	1
	Moderate	Three-axis task, no collective, control harmony good. Desired performance achieved satisfactorily. Minimal control activity. Lots of spare capacity. Using only small inputs to keep on target.	2	1
Lateral jinking	Low	Single-axis task, good tracking. Nice crisp roll response. Task workload minimal.	2	1
	Moderate	Tracking directly down lines, no coupling. Moderate aggression does not do it justice. Task workload minimal to moderate. Control law really good at this task. Coupling: none. Desired performance easily achieved. Influencing factors: primary response and coupling, positive. Inceptor, negative.	2	1

end of which the simulation was paused so that comments and handling qualities ratings (HQRs) could be recorded. HQRs of 1, 2, and 3 equate to level-1 flying qualities on the Cooper–Harper scale, whereas HQRs of 4, 5, and 6 equate to level-2 flying qualities. HQRs of 7, 8, and 9 equate to level 3. An HQR of 7 or worse implies that there are major handling deficiencies.

Pilot Comment

During the first trial in May, pitch and roll attitude control was considered excellent by both pilots, who awarded 11 HQRs of 2 (in one case a low 2, the pilot felt that he could not award an HQR of 1 on the basis of a simulator test alone) and 1 HQR of 3 for pitch and roll control tasks. Both pilots found the stability quite impressive; they were able to take their hands totally off the controls at hover. One pilot commented after completing side-step tasks that "flying conventional Lynx models, there is no way you can achieve the sort of accuracy you can with this with such a low workload." The roll axis response was described as perfect. Both pilots felt that, during the roll axis task, increased levels of aggressiveness did not result in an increased workload. Excessive heave-to-yaw coupling and a sluggish heading rate response, however, resulted in HQRs of 3, 4, and 5 for heave axis control tasks, and HQRs of 5 and 7 in the yaw pointing task. Subsequent investigation revealed that these problems arose because the original SRM had 1) too high a heave-axis bandwidth, leading to saturation of the main rotor collective, thereby compromising the decoupling properties of the controller; and 2) too low a heading axis bandwidth. This was remedied by a redesign incorporating the SRM described in this paper. This meant simply changing the SRM parameters and recomputing the controller. Pitch and roll axes were left essentially unaltered.

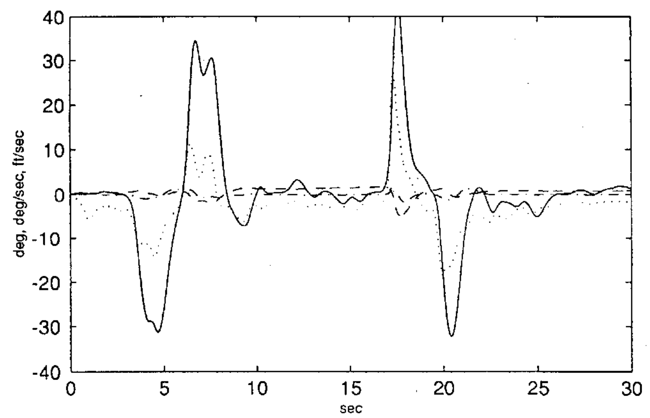

Fig. 11 Lateral jinking data: —·—, heave velocity; – – –, pitch attitude; ——, roll attitude; and ·····, heading rate.

The resulting redesign was then rigorously tested toward the end of December 1992. Only one pilot was able to participate in that trial. His comments are summarized in Table 9.

The control law had not been designed to regulate or in any way limit torque. Note how the rating dropped when the pilot was required to close the torque loop manually. Investigations into carefree handling control systems by Howitt[18] suggest that this problem can be solved.

Data from Piloted Trial

Rigid body states, torque, rotor speed, inceptor movement, and control actuator activity were logged during several of the runs. A sample of the data is reproduced in Fig. 11. There was some evidence of inceptor couplings between pitch and roll; on numerous occasions, the pilot cited the inceptor as a negative-influencing factor. Otherwise, the cross couplings are minimal and the performance well within specification.

Conclusions

A 2-DOF multivariable controller was designed using a model of the Lynx. It was extensively tested on the LMS at the DRA, Bedford. Although the controller had been designed for hover and low speed, it remained fully functional at speeds in excess of 100 kn. Degradation in performance over the range 0–60 kn was minimal, indicating robust performance. Through this study we have demonstrated the assimilation of specific handling qualities requirements direct from a specification into the control law design. This has been achieved via a 2-DOF H^∞ optimization leading to robust stability and robust model following. The possibility of synthesizing a controller accurately replicating the responses of the model in the closed loop was confirmed during this study. This has proved to be an effective mechanism for incorporating basic quantitative handling quality requirements into the design process.

The resulting high bandwidth attitude command response gave almost total decoupling between the controlled outputs. Interaxis couplings were suppressed to well below the 25% required by the Military Rotorcraft Handling Qualities Specification. During the piloted simulations, level-1 Cooper–Harper pilot ratings were consistently achieved during aggressively performed mission task elements. Precision tasks were successfully completed with minimal pilot workload. Robust stability over a wide part of the modeled flight envelope has been demonstrated.

The control law was tuned with a view to exploring through simulation what might in principle be feasible with the aircraft. Considerable work remains to be done before such a controller is flight tested. For instance, during the trials certain vehicle limits were exceeded. These included lateral velocity, side slip, and torque. Torque protection could be incorporated using a simple outer-loop feedback. As for the flight-envelope limitations, these are not a direct consequence of the controller design, but rather inherent limitations in the aircraft's performance envelope. The handling qualities and workload improvements associated with the controller simply gave the test pilots greater scope and confidence in exploring these limits. For further developments to take place, appropriately validated simulation models containing higher order dynamics will be required.

One linear time-invariant controller may in practice not be adequate for full-envelope control on an aircraft such as the Lynx. A scheduling method based on interpolation of several controllers designed at different operating points has also been implemented. Investigations are ongoing as to what controller scheduling offers in terms of wide envelope operation, stability, and performance.

Acknowledgments

This work was conducted with the support of the UK Ministry of Defence through Extramural Research Agreement 2206/32/RAE(B). The authors wish in particular to thank Jeremy Howitt, S. Cheyne, and P. Sharpe of DRA Bedford, who were all instrumental in the testing and assessment of the control law.

References

[1]Yue, A., and Postlethwaite, I., "Improvement of Helicopter Handling Qualities Using H^∞ Optimisation," *IEE Proceedings*, Pt. D, Vol. 137, 1990, pp. 115–129.

[2]Walker, D. J., and Postlethwaite, I., "Full Authority Active Control System Design for a High Performance Helicopter," *Proceedings of the 16th European Rotorcraft Forum*, Royal Aeronautical Society, London, 1990, pp. III.3.2.1–III.3.2.14.

[3]Maclay, D., and Howitt. J., "Design and Handling Qualities Analysis of a Full Envelope Multivariable Controller for a Combat Rotorcraft," *Aerospace Vehicle Dynamics and Control*, Clarendon, Oxford, England, UK, 1994, pp. 181–198.

[4]Gribble, J. J., "Linear Quadratic Gaussian/Loop Transfer Recovery Design for a Helicopter in Low-Speed Flight," *Journal of Guidance, Control, and Dynamics*, Vol. 16, No. 4, 1993, pp. 754–761.

[5]Anon., "Handling Quality Requirements for Military Rotorcraft ADS-33C," U.S. Army Aviation Systems Command, St. Louis, MO, 1989.

[6]Howitt, J., "MATLAB Toolbox for Handling Qualities Assessment of Flight Control Laws," *IEE International Conference on CONTROL '91* (Edinburgh, Scotland, UK), IEE Conference Publications, London, 1991, pp. 1251–1256.

[7]Francis, B. A., *A Course in H^∞ Control Theory*, Lecture Notes in Control and Information Science, Springer–Verlag, Berlin, 1987.

[8]Vidyasagar, M., *Control System Synthesis—A Factorization Approach*, MIT Press, Cambridge, MA, 1985.

[9]Padfield, G. D., "A Theoretical Model of Helicopter Flight Mechanics for Application to Piloted Simulation," TR RAE TR 81048, Royal Aircraft Establishment, Farnborough, England, UK, 1981.

[10]Howitt, J., and Cheyne, S., "Assessment of the DRA Helisim Lynx Math Model on the DLR BO105 (ATTHeS) In-Flight Simulator," Defence Research Agency, DRA Working Paper WP(92) 046, Bedford, England, UK, July 1992.

[11]Hoyle, D., Hyde, R., and Limebeer, D., "An H^∞ Approach to Two Degree of Freedom Design," *Proceedings of the 30th IEEE Conference on Decision and Control*, Inst. of Electrical and Electronics Engineers, Piscataway, NJ, 1991, pp. 1581–1585.

[12]McFarlane, D., and Glover, K., *Robust Controller Design Using Normalized Coprime Factor Plant Descriptions*, Lecture Notes in Control and Information Science, Springer–Verlag, Berlin, 1990.

[13]Kouvaritakis, B., "Characteristic Locus Methods for Multivariable Feedback Systems Design," Ph.D. Thesis, Dept. of Electrical Engineering, Univ. of Manchester IST, Manchester, England, UK, 1974.

[14]Walker, D. J., "On the Structure of a Two-Degree-of-Freedom H^∞ Loop Shaping Controller," *International Journal of Control* (to be published).

[15]Lehtomaki, N., Sandell, N., and Athans, M., "Robustness Results in Linear-Quadratic Gaussian Based Multivariable Control Designs," *IEEE Transactions on Automatic Control*, Vol. AC-26, No. 1, 1981, pp. 75–93.

[16]Padfield, G. D., Charlton, M. T., and Kimberley, A. M., "Helicopter Flying Qualities in Critical Mission Task Elements—Initial Experience with the DRA (Bedford) Large Motion Simulator," *Proceedings of the 18th European Rotorcraft Forum* (Avignon, France), Association Aeronautique et Astronautique de France, Paris, 1992, pp. F2-1–F2-36 (Paper F2).

[17]Osder, S., and Caldwell, D., "Practical Robustness Testing for Helicopter Flight Control Systems," *Proceedings of the 47th American Helicopter Society Annual Forum*, 1991, American Helicopter Society, Alexandria, VA, pp. 209–221.

[18]Howitt, J. "Carefree Maneuvering in Helicopter Flight Control," *Proceedings of the 51st American Helicopter Society Annual Forum* (Fort Worth, TX), American Helicopter Society, Alexandria, VA, 1995, pp. 287–298.